Damped Pseudospectral Functional Forms of the Falloff Behavior of Unimolecular Reactions

Prasana K. Venkatesh

Schlumberger-Doll Research, Old Quarry Road, Ridgefield, Connecticut 06877

Received: May 4, 1999; In Final Form: October 20, 1999

The competition between thermalization and dissociation in dilute gas-phase unimolecular reactions gives rise to absolute rate constants as a function of temperature and the number density. Such competitive effects are fully modeled using a master equation formalism that accounts for conservation of total angular momentum as well as conservation of total energy. After such modeling, a general functional form of the rate constants is necessary for approximating the temperature- and pressure-dependent behavior. We present a damped pseudospectral functional form for such an approximation. It is a computationally efficient and an highly accurate approximation. We illustrate the method and demonstrate its advantages by application. Comparison with extant methods of approximation is also given. Given applications pertain to a singe-well, single-channel reaction, which allows for radiative recombination of radicals in interstellar chemistry, to a single-well, multiple-channel chemically activated reaction in chemical vapor deposition, and, a multiple-well, multiple-channel chemically activated reaction in combustion.

1. Introduction

Quantum statistical methods, such as the Rice−Ramsperger−Kassel−Marcus (RRKM) theory,[1−3] have been proved to be accurate in estimating the microcanonical rate coefficients of many gas-phase elementary reactions in combustion, atmospheric chemistry, and chemical vapor deposition. In conjunction with a suitable model of intermolecular collisions, such as a full master equation treatment, an absolute rate constant may be derived.[4,5] The knowledge of such temperature- and pressure-dependent rate constants is very important in constructing predictive gas-phase chemical reactor models using mechanistic chemical reaction schemes; these are schemes which consist of a vast number of elementary reactions.

Approximation of absolute rate constants is very important in simulation and optimization of chemical reactors and in computational fluid dynamics of reactive flows. For instance, simulation and optimization of chemical reactors in vapor deposition and combustion require repeated computations of rate constants of each elementary reaction of the chemical kinetic schemes as a function of the controlling parameters over wide ranges of temperature and pressure. It is computationally inefficient to invoke an RRKM master equation computation each time such values of the rate constant are desired. Inference of these values from an approximant which is both accurate and computationally efficient is the optimum manner of incorporating pressure dependence and temperature dependence of elementary reactions in complex chemical kinetic schemes.

There have been many efforts to devise accurate approximations of the falloff behavior of thermally- and chemically activated unimolecular reactions beginning with Lindemann's seminal enunciation in the nineteen-twenties. Of recent importance are the methods due to Troe and co-workers for the treatment of single-well, thermally activated unimolecular reactions.[6,7] These methods have been specifically developed for simple dissociation and recombination reactions proceeding through a single well. In such reactions, the absolute rate constants are very sensitive to pressure in the low-pressure and falloff regimes. These methods of approximation, although accurate for single-well reactions, do not apply well to multiple-well unimolecular reactions as shown in a recent detailed study of several sets of unimolecular reactions.[8] Chemically activated reactions, in particular, exhibit pressure-dependent behavior which is qualitatively and quantitatively different from that exhibited by single-well dissociation or recombination reactions.[6−8]

Multiple-well unimolecular reactions are ubiquitous in the engineering of chemical reactions, particularly, in combustion. In ref 8, a method based on pure Tchebycheff expansions was presented for accurately approximating the falloff behavior of unimolecular reactions proceeding through any number of isomerization and dissociation channels over wide ranges of temperature and pressure.

In this paper we present a damped pseudospectral functional form for approximating the temperature- and pressure dependence of the absolute rate constants. This method, which is related to the Tchebycheff approximation, is superior to pure Tchebycheff expansions in several ways. First, it allows the falloff surface, which is a function of temperature and pressure, to possess arbitrary discontinuities in any of its derivatives, in other words, the falloff function is not required to be entire[9] for conduciveness to efficient and accurate approximation; here we note that an entire function is one for which its derivatives of any order are continuous functions. Second, for the same number of parameters, it provides approximants of higher accuracy than a pure Tchebycheff expansion.

The advantages of the damped pseudospectral functional form developed in this paper are demonstrated by application to approximation of the falloff behavior of three systems of reactions. The first, a single-well, single-channel system, is the recombination reaction of the hydrogen atom with the C_6H_5 radical allowing for radiative recombination[10] due to infrared emission. The second is the single-well, multiple-channel, chemically activated reaction of $SiHCl + SiH_2Cl_2$.[11,12] The third

10.1021/jp991458u CCC: $19.00

is the multiple-well, multiple-channel, chemically activated system of reactions of the association of oxygen with the ethyl radical.[5,13] The falloff behaviors of these reactions were determined by computing the absolute rate constants from a full master equation analysis[4,5] in conjunction with a full RRKM treatment which includes the conservation of angular momentum in addition to the conservation of total energy available for randomization.

The remainder of the paper is organized as follows. Section 2 briefly presents the essentials of directly computing the temperature- and pressure dependence of absolute rate constants of gas-phase unimolecular reactions within the framework of transition state theory and recent developments in master equation analysis. Section 3 develops the damped pseudospectral functional fitting form. Section 4 presents comparisons of the accuracy of the damped pseudospectral functional fitting form for three systems of reactions with extant methods of approximating the falloff behavior. Finally, section 5 gives a summary of our findings.

2. Preliminaries: Temperature and Pressure Dependent Rate Constants

We begin by summarizing the essential theoretical aspects pertaining to the derivation of temperature- and pressure-dependent rate coefficients for unimolecular reactions in the gas phase. It is the functional dependence of these rate constants on temperature and pressure which we seek to approximate by the damped pseudospectral functional form presented in section 3.

The physical system of concern is described as follows. We consider, most generally, irrespective of the form of activation, multiple-well unimolecular reactions in a concentrated bath consisting of N reactive moieties

$$A_1, A_2, ..., A_N \tag{2.1}$$

where N is the total number of wells. Associated with each well is a particular moiety and each moiety may isomerize to any of its $N - 1$ counterparts. For illustrative purposes, it may simply be assumed that A_1 is the entrance isomer formed by some process of activation − thermally, chemically, or otherwise. Each moiety undergoes collisions with the gaseous bath of a number density $[M]$. The moieties may take the form of an unsaturated molecule or a radical.

Also, each moiety may dissociate into products via a finite number of product channels pertinent to the well specific to it. For each product channel, the ultimate quantity of interest is the absolute rate constant $k(T, P)$ of product formation. In addition to being a function of temperature T, this quantity is a function of pressure P due to the competition between the collision of the moiety A_i with the bath gas and its dissociation into products; here i is the index variable specifying the pertinent well. It is the functional dependence of $k(T, P)$ on T and P which we seek to approximate by the damped pseudospectral functional form presented in section 3. There are two aspects to the theoretical determination of the absolute rate constant $k(T, P)$: that of computing microcanonical rate coefficients $k(E, J)$ and that of computing the effects of intermolecular collisions of moieties with the bath gas of number density $[M]$.

The microcanonical rate coefficients, $k(E, J)$, are functions of the total randomization energy E and the angular momentum quantum number J. They may be computed using any version of transition state theory, including RRKM theory[1] and variational-RRKM theory[2], phase space theory,[14] statistical adiabatic channel model,[15] variationally adiabatic transition state theory,[16] and, whenever computationally feasible, even by semiclassical and quantum mechanical treatments of transition state theory.[17] In the computations described herein we determine the microcanonical rate coefficients

$$k(E, J) = \frac{G(E, J)}{h\rho(E, J)} \tag{2.2}$$

by employing variational-RRKM theory. Here $G(E, J)$, which is variationally determined, is the number of quantum states of the transition state at the particular E and J, $\rho(E, J)$ is the density of states of the parent molecule with vibrational anharmonicity taken into account whenever practical, and h is Planck's constant.

In the absence of a full quantitative theory of intermolecular collisions, the effects of intermolecular collisions of the moieties with the bath gas are best determined from a master equation analysis.[18] At each state of the total energy E and the total angular momentum quantum number J there will be a certain population of each of the N moieties. The state-specific population will dynamically change due to interwell energy transfer, when there is more than one well, due to isomerization and intrawell energy transfer due to collisions with the bath gas within each well. A set of conservation equations for the dynamics of the moieties' populations over each state subject to interwell and intrawell transfer may be simply derived and collectively forms a master equation. The master equation can then be analyzed to derive the state-specific population of the moieties $[A_i(E, J; [M], t)]$, $1 \le i \le N$.

The master equation may be written down most generally, irrespective of the form of activation, as

$$\frac{\partial}{\partial t}[A_{\mathrm{i}}(E, J; [M], t)] = \sum_{j=1}^{N} \sum_{J'=0}^{\infty} \int_0^{\infty} \langle iEJ|\kappa|jE'J'\rangle [A_j(E', J'; [M], t)]\mathrm{d}E' + U_i(t) \quad 1 \le i \le N \tag{2.3}$$

Here, the master equation kernel κ is composed of microcanonical rate coefficients which account for the three fundamental reactions that each of the moieties may undergo: dissociation of each moiety into stable products, isomerization of each moiety into any one of the other $N - 1$ moieties, and thermalization of each moiety with the bath gas. The internal spectrum of the master equation kernel represents the time scales of the dynamics of thermalization within each of the wells, of isomerization over all of the wells, and of dissociation within each of the wells. $U(t) \equiv [U_1(t), ..., U_N(t)]$ denotes an inhomogeneous source term that is a function of time and takes appropriate functional forms depending on the kind of the activation of reaction (thermal or chemical). For chemically activated reactions, $U_i(t)$ denotes the rate of formation of the ith moiety $[A_i(E, J; [M], t)]$ from the chemically activated reactants; in this case $U_i(t)$ will be state-specific, that is, it will be a function of the total internal energy E as well as the total angular momentum quantum number J. For thermally activated reactions, $U_i(t)$ denotes the contribution of the thermally activated flux to the ith moiety $[A_i(E, J; [M], t)]$, and it may or may not be state specific.

That one can identify rate equations which are local in time for the dissociation processes only in a regime of secular equilibrium state was rigorously established in ref 4 where it was also shown that there may exist a subregime wherein the existence of a nontrivial least-negative eigenvalue separated in magnitude from the time scales of thermalization is possible. The condition for the occurrence of secular equilibrium has nothing to do with the internal spectrum of the master equation kernel but rather with the magnitude of the least-negative eigenvalue relative to the time rate of change of the inhomogeneous term of the master equation. The existence of a state of secular equilibrium is established by inquiring the validity of the condition given by

$$\left|\frac{1}{U_{\lambda_k}(t)}\frac{\partial}{\partial t}U_{\lambda_k}(t)\right| \ll |\lambda_k| \quad 1 \le k < \infty \tag{2.4}$$

where

$$U_{\lambda_k}(t) = \sum_{J=0}^{\infty} \int_0^{\infty} \phi_{\lambda_k}(E, J) U(t) \mathrm{d}E \quad 1 \le k < \infty \tag{2.5}$$

with λ_k being the kth eigenvalue of the kernel κ, and $\phi_{\lambda k}(E, J)$ being the associated adjoint eigenfunction of κ. Very efficient means of numerically verifying the conditions of the validity of the state of secular equilibrium, analysis of the internal spectrum of the master equation kernel, and computation of the moiety populations $[A_i(E, J; [M], t)]$, $1 \le i \le N$ using Hermite−Laguerre orthogonal collocation have recently been established.[5]

The population, $[A_i(E, J; [M], t)]$, of the moiety A_i, for a particular E, J, and number density $[M]$, at time t along with the microcanonical rate coefficient $k(E, J)$ of product formation pertaining to well i are related to the absolute temperature- and pressure-dependent rate constant of product formation for the attendant well by

$$k(T, P) = \frac{\sum_{J=0}^{\infty} \int_0^{\infty} k(E, J)[A_\mathrm{i}(E, J; [M], t)] \mathrm{d}E}{\sum_{J=0}^{\infty} \int_0^{\infty} [A_\mathrm{i}(E, J; [M], t)] \mathrm{d}E} \tag{2.6}$$

It is the functional dependence of these rate constants on temperature and pressure which we seek to approximate by the damped pseudospectral functional form presented in section 3.

3. A Damped Pseudospectral Functional Form for *k*(*T*, *P*)

The starting point for the development is the Tchebycheff polynomial representation given in ref 8 which considers the direct approximation of the logarithm of the absolute rate coefficients $k(T, P)$ of eq 2.6 in terms of the inverse temperature and logarithm of the pressure. Given the ranges of temperature and pressure over which approximation of the rate coefficients are desired,

$$T_\mathrm{min} \le T \le T_\mathrm{max} \tag{3.1}$$

and

$$P_\mathrm{min} \le P \le P_\mathrm{max} \tag{3.2}$$

a mapping of the temperature and pressure domain onto the unit square is first performed by the transformations

$$T \leftarrow \frac{2T^{-1} - T_\mathrm{min}^{-1} - T_{max}^{-1}}{T_\mathrm{min}{}^{-1} - T_\mathrm{max}{}^{-1}} \tag{3.3}$$

and

$$P \leftarrow \frac{2\log P - \log P_\mathrm{min} - \log P_\mathrm{max}}{\log P_\mathrm{max} - \log P_\mathrm{min}} \tag{3.4}$$

in order to scale the temperature and pressure to vary between minus one and plus one. This scaling procedure does not alter the values of the rate coefficient in any way. The logarithm (which may be fixed to a certain convenient base, e.g., 10) of the rate coefficient is thus approximated as

$$\log k(T, P) \approx \sum_{n=1}^{N} \sum_{m=1}^{M} a_\mathrm{nm} \varphi_n(T) \varphi_m(P) \tag{3.5}$$

where the Tchebycheff polynomial of the first kind of degree n − 1 is given by

$$\varphi_n(x) = \cos((n - 1)\ \mathrm{acos}(x)) \quad \mathrm{n} = 1, 2, ... \tag{3.6}$$

and where x is the argument of interest defined to lie in the closed interval $[-1, +1]$. Here, the integer N denotes the number of basis functions along the temperature axis, the integer M denotes the number of basis functions along the pressure axis, and the $\{a_{nm};\ 1 \le n \le N,\ 1 \le m \le M\}$ are the NM coefficients to be determined from a set of data points at which the rate coefficients, $k(T, P)$, have been computed exactly from a detailed theory by eq 2.6. The data points at which the rate coefficients $k(T, P)$ are computed for the estimation of a_{11}, a_{12}, ..., a_{nm}, ..., a_{NM} should be the roots of a high-order Tchebycheff polynomial of the first kind. Such a grid of data points is termed as the Gauss−Tchebycheff grid. This is necessary to ensure that the approximation is uniform over the whole domain of the temperature and pressure interval. The integers, N and M, are chosen in advance. Their choice serves to control the accuracy of the approximant, which increases monotonically with N and M. The rate coefficients, $k(T, P)$, may be computed on a $d_T \times d_P$ Gauss−Tchebycheff grid. This grid is given by

$$T_i = \cos\left[\frac{2i - 1}{2d_T}\pi\right] \tag{3.7}$$

$$P_j = \cos\left[\frac{2j - 1}{2\mathrm{d}_P}\pi\right] \tag{3.8}$$

$$1 \le i \le d_T \text{ and } 1 \le j \le d_P \tag{3.9}$$

N and M can be varied to construct approximants of different orders of accuracy. In the development presented in ref 8, the coefficients $\{a_{nm};\ 1 \le n \le N,\ 1 \le m \le M\}$ were obtained by least-squares estimation by minimizing the expression

$$\sigma^2(a_{11}, ..., a_{NM}) = \frac{\pi^2}{d_T d_P} \sum_{i=1}^{d_T} \sum_{j=1}^{d_P} [\log k(T_\mathrm{i}, \mathrm{P_j}) - \sum_{n=1}^{N} \sum_{m=1}^{M} a_{nm} \varphi_n(T_i) \varphi_m(P_j)]^2 \tag{3.10}$$

which fits eq 3.5 to the values of log $k(T, P)$ obtained from eq 2.6 evaluated over the $d_T \times d_P$ Gauss−Tchebycheff grid of equations (3.7−3.9). Needless to say, for such a calculation, to obtain an overdetermined system, $d_T d_P > NM$ is a necessary condition.

At this juncture we are now ready to introduce the new development. We now propose that the expression denoting the approximation of eq 3.5 be replaced by

$$\log k(T, P) \approx \sum_{n=1}^{N}\sum_{j=1}^{M} S_{\mathrm{nm}}(N, M) a_{\mathrm{nm}} \varphi_{\mathrm{n}}(T)\varphi_{m}(P) \quad (3.11)$$

Here$\{S_{nm}(N, M);\ 1 \le n \le N,\ 1 \le m \le M\}$ is an attenuation factor and all other symbols retain their previously defined meanings. We also propose that the NM coefficients $\{a_{nm};\ 1 \le n \le N,\ 1 \le m \le M\ \}$ be computed by the transform

$$a_{nm} = \frac{4}{\pi^2}\int_{-1}^{1}\int_{-1}^{1} \log k(T, P)\, \frac{\varphi_n(T)\varphi_m(P)}{\sqrt{1 - T^2}\,\sqrt{1 - P^2}}\mathrm{d}P\mathrm{d}T$$
$$1 \le n \le N, 1 \le m \le M \quad (3.12)$$

which is exactly a bivariate Fourier cosine transform with respect to an appropriate change of variables in temperature and pressure. This manner of evaluating the coefficients $\{a_{11}, a_{12}, ..., a_{nm}, ..., a_{NM}\ \}$ is vastly more accurate and computationally simpler than the least-squares minimization of eq 3.10. The numerical evaluation of eq 3.12 is performed most accurately by application of the Gauss−Tchebycheff quadrature over the $d_T \times d_P$ Gauss−Tchebycheff grid of equations (3.7−3.9). The quadrature formula[19] is then written as

$$a_{nm} = \frac{4}{d_T d_P}\sum_{i=1}^{d_T}\sum_{j=1}^{d_P} \log k(T_{\mathrm{i}}, \mathrm{P}_{\mathrm{j}})\varphi_n(T_{\mathrm{i}})\varphi_m(P_{\mathrm{j}})$$
$$1 \le n \le N, 1 \le m \le M \quad (3.13)$$

and we note that there is no particular constraint relating the values of d_T and d_P to the values of N and M. However, we note that as the values of d_T and d_P are increased, the difference between representations of eqs 3.12 and 3.13 rapidly approaches zero.

The second significant difference between the approximant of eq 3.11 and the one of eq 3.5 is the introduction of attenuation factors $\{S_{nm}(N,M);\ 1 \le n \le \mathrm{N},\ 1 \le m \le M\}$. The attenuation factors are very important. They prevent spurious oscillations in the approximated rate coefficient; additionally, they enable faster convergence to the true function with fewer terms in the series expansion as well as accurately capturing any sharp and sudden changes of the surface representing the absolute rate constant $k(T, P)$. Spurious oscillations occur because of the truncation in eq 3.5 in order to retain only a finite number, NM, of basis functions. To prevent such oscillations each term of eq 3.5 must be attenuated. Each attenuation factor is a function of the total numbers, N and M, of the retained bases.

The next step is the construction of the NM attenuation factors $\{S_{nm}(N, M);\ 1 \le n \le \mathrm{N},\ 1 \le m \le M\}$. This is done by formulating a mathematical problem of optimization in a space of NM degrees of freedom.[19] Constraints may then be imposed in order to reduce the degrees of freedom. Particular constraints that need be imposed are the positivity of the approximated rate coefficient at each point in the temperature and pressure domains and the approximation of sharp features with minimal smearing or broadening. The latter issue is best addressed by computing the best approximation of a Dirac-delta function in a minimax sense, i.e., we seek an approximation to a bivariate delta function which minimizes the maximum deviation of the approximant from the true delta function over the entire temperature and pressure domains. This minimax optimization is performed by optimizing over the available degrees of freedom. Fortunately, an analytical solution exists[19] to this problem of constructing attenuation factors by minimax optimization.

Minimax theory[19] allows us to construct such an optimum attenuation factor as follows. We separate the attenuation factors along the temperature and pressure axes in a multiplicative fashion as

$$S_{nm}(N, M) = \chi_T(n, N) \times \chi_{\mathrm{P}}(m, M) \quad (3.14)$$

The computation of the attenuation factors is based on the Tchebycheff polynomials of the second kind which are given by

$$\psi_i(x) = \frac{\sin(i\operatorname{acos}(x))}{\sin(\operatorname{acos}(x))} \quad \mathrm{i} = 1, 2, ... \quad (3.15)$$

where x is the argument of interest. The attenuation factor along the temperature axis may be computed as

$$\chi_T(n, N) = \sum_{l=1}^{N-n+1} \alpha(l, N) \times \alpha(l + n - 1, N) \quad 1 \le n \le N \quad (3.16)$$

with

$$\alpha(l, N) = \frac{\psi_l(\pi/(N + 1))}{\sqrt{\sum_{i=1}^{N}[\psi_i(\pi/(N + 1)) \times \psi_i(\pi/(N + 1))]^2}} \quad (3.17)$$

Equation 3.16 may be simplified and the following expression may be derived

$$\chi_T(n, N) = \Big[\frac{N - n + 2}{N + 1}\sin\frac{\pi}{N + 1}\cos\pi\frac{n - 1}{N + 1} + \frac{1}{N + 1}\cos\frac{\pi}{N + 1}\sin\pi\frac{n - 1}{N + 1}\Big]/\sin\pi/(N + 1) \quad (3.18)$$

Similarly, for the pressure axis, the attenuation factor may be computed as

$$\chi_P(m, M) = \sum_{l=1}^{M-m+1} \alpha(l, M) \times \alpha(l + m - 1, M)$$
$$1 \le m \le M \quad (3.19)$$

and it may be derived that

$$\chi_P(m, M) = \Big[\frac{M - m + 2}{M + 1}\sin\frac{\pi}{M + 1}\cos\pi\frac{m - 1}{M + 1} + \frac{1}{M + 1}\cos\frac{\pi}{M + 1}\sin\pi\frac{m - 1}{M + 1}\Big]/\sin\pi/(M + 1) \quad (3.20)$$

To recapitulate, the damped pseudospectral approximant to the temperature- and pressure-dependent rate coefficients of eq 2.6 is given by eq 3.11. It requires the computation of NM basis coefficients $\{a_{11}, a_{12}, ..., a_{\mathrm{nm}}, ..., a_{NM}\}$ as well as the NM attenuation factors $\{S_{11}(N, M), S_{12}(N, M), ..., S_{nm}(N, M), ..., S_{NM}(N, M)\}$. N and M are appropriately chosen to yield an approximant of *any* desired accuracy. The basis coefficients are computed using the quadrature formula of eq 3.13 and the attenuation factors are determined by the minimax formulas given by eqs 3.14, 3.18, and 3.20.

4. Applications

The criterion of assessment of the approximation scheme considered here is based on the maximum and average relative errors in the approximated rate coefficient over the entire temperature and pressure domain. The relative error is defined as

TABLE 1: Maximum Relative Errors in the Rate Coefficient over the Considered Temperature and Pressure Ranges for Empirical Approximants with Master Equation Analysis of the Collisional Energy Transfer[a]

	Method	
channel	Troe (F_{cent})	Poole and Gilbert
Single-Well, Single-Channel $H + C_6H_5 \rightarrow C_6H_6$ Reaction with Allowance for Radiative Recombination		
$H + C_6H_5 \rightarrow C_6H_6$	0.3 (0.17)	0.19 (0.13)
Single-Well, Multiple-Channel Reaction of $SiHCl + SiH_2Cl_2$		
$SiH_2 + SiHCl_3$	0.18 (0.09)	0.10 (0.08)
$SiHCl + SiH_2Cl_2 \rightarrow SiCl_2 + SiH_3Cl$	1.8 (0.4)	0.8 (0.42)
$SiHCl + SiH_2Cl_2 \rightarrow Si_2HCl_3 + H_2$	3.2 (1.1)	0.33 (0.17)
Multiple-Well, Multiple-Channel Reaction of the Ethyl Radical with Oxygen [first (entrance) well pertaining to the formation of the chemically activated moiety]		
$CH_3CH_2O\dot{O} \rightarrow C_2H_5\dot{O} + O$	0.17 (0.12)	0.1 (0.07)
$CH_3CH_2OO \rightarrow C_2H_4 + HO_2$(elimination)	0.42 (0.23)	0.26 (0.17)
Second well pertaining to the first hydroperoxy radical and β scission pathway:		
$\dot{C}H_2CH_2OOH \rightarrow C_2H_4 + HO_2$($\beta$ scission)	4.4 (1.5)	0.33 (0.19)
$\dot{C}H_2CH_2OOH \rightarrow$ (cy)$H_2COCH_2 + OH$	0.98 (0.72)	0.31 (0.17)
Third Well Pertaining to the Second Hydroperoxy Radical and Formation of Acetaldehyde		
$CH_3\dot{C}HOOH \rightarrow CH_3CHO + OH$	0.1 (0.06)	0.15 (0.08)

[a] The numbers in parentheses indicate average errors in the rate coefficient.

$$\text{relative error} = \left|1 - \frac{[k(T,P)]_{\text{approx}}}{[k(T,P)]_{\text{theoretical}}}\right| \qquad (4.1)$$

Here, in eq 4.1, the subscript approx refers to the approximant of the absolute rate constant. The subscript theoretical refers to the absolute rate constant obtained from a detailed theoretical calculation. In our study, the detailed theoretical calculations of the rate constants are based on a variational RRKM theory for the microcanonical rate coefficients and a full master equation treatment, including the conservation of angular momentum, for the treatment of intermolecular collisional effects.[4,5] Without loss of generality, we consider an approximant to be reliably accurate if it yields a relative error of no more than 0.2 over the entire temperature and pressure. In this study we adopt this measure of goodness of approximation in comparing the various approximation schemes analyzed.

It was confirmed in ref 8 that the presence of multiple wells and the occurrence of multiple products in a chemically activated reaction or dissociation reaction leads to complex temperature and pressure dependences. This was demonstrated on a select set of three dissociation channels pertaining to the dissociation of the $C_3H_5O_2$ radical and ethane, and four chemical-activation channels pertaining to the reaction of the allyl radical with molecular oxygen and that of the methyl radical with itself. In particular, it was shown that on the multiple-well dissociation channel $C_3H_5O_2 \leftrightarrow C_3H_5 + O$ and the single-well channels corresponding to the dissociation of ethane the Lindemann-based methods yielded maximum relative errors greater than 0.2 for approximation over the wide temperature and pressure ranges of 300−3000 K and 0.02−200 atm. In the same study it was demonstrated that the chemical-activation reactions considered could not be fitted to acceptable accuracy by the conventional approximation methods for the same ranges of temperature and pressure. A definitive conclusion was drawn from this study that conventional approximation schemes are inadequate for multiple-well, multiple-product dissociation and chemical activation reactions.

In this study we present comparisons of various approximation schemes by focusing on three systems of reaction. For each system of reaction we compare the following approximation schemes: Troe's F_{cent} method as described in ref 6, the scheme due to Poole and Gilbert as described in ref 7, the pure Tchebycheff scheme as described in ref 8, and the damped pseudospectral scheme described in section 3. For the comparisons, we have computed the absolute rate coefficients of all of the reactions on a 50 × 50 temperature−pressure grid over the entire considered domain of temperature and pressure; for each system of reaction, the considered domain is different and will be specified shortly. This grid is equidistant for all of the approximation schemes considered here with the exception of Tchebycheff and damped pseudospectral approximations which require a specially chosen nonequidistant grid, the description of which has been given in section 3. Tables 1−3 present the results of the four methods of approximation considered over all three systems of reactions. Both the maximum errors and average errors incurred over the entire temperature and pressure domains are tabulated.

The first system of reaction is one of importance in interstellar chemistry. It is the recombination of the H atom with the C_6H_5 radical. At low and moderate temperatures infrared radiative stabilization in the ground state is critical in enhancing the efficiency of reaction. A full variational RRKM treatment in conjunction with the full master equation analysis laid out in ref 4 was undertaken for this recombinative reaction with respect to an argon bath. Spontaneous emission Einstein coefficients were determined from the infrared transition intensities available in the literature (ref 10 and references therein). Absolute rate constants were calculated for the temperature and pressure ranges of 20−2000 K and $2 \times 10^{-10} - 2 \times 10^{-3}$ atm. Tables 1−3 present the maximum and average errors of approximation for these channels incurred by the Lindemann-based empirical approximants, the Tchebycheff approximants, and the damped pseudospectral approximants, respectively, for this reaction.

The second system of reactions is one of importance in chemical vapor deposition. It is the chemically activated reaction of $SiHCl + SiH_2Cl_2$ which proceeds via the formation of the moiety HCl_2SiSiH_2Cl to decompose into three product channels. The moiety may also reversibly decompose into the reactants. This system of reactions has been well studied[11,12] using a full RRKM treatment in conjunction with the full master equation treatment given in refs 4 and 12 in these studies, the thermal bath was taken to be one of gaseous hydrogen. Table 4 displays the limiting high-pressure rate coefficients for the various channels of this reaction. For these channels, we have compared the various models of approximation over the wide temperature- and pressure ranges of 300−3000 K and 2×10^{-5}−200 atm.

TABLE 2: Maximum Relative Errors in the Rate Coefficient over the Considered Temperature and Pressure Ranges for the Tchebycheff Approximants with Master Equation Analysis of the Collisional Energy Transfer[a]

channel	6 × 3	5 × 4	7 × 3	6 × 4	8 × 3
Single-Well, Single-Channel $H + C_6H_5 \rightarrow C_6H_6$ Reaction with Allowance for Radiative Recombination					
$H + C_6H_5 \rightarrow C_6H_6$	0.15 (0.12)	0.15 (0.11)	0.12 (0.09)	0.08 (0.06)	0.06 (0.05)
Single-Well, Multiple-Channel $SiHCl + SiH_2Cl_2$ reaction					
$SiHCl + SiH_2Cl_2 \rightarrow SiH_2 + SiHCl_3$	0.09 (0.05)	0.09 (0.04)	0.06 (0.03)	0.04 (0.02)	0.01 (0.01)
$SiHCl + SiH_2Cl_2 \rightarrow SiCl_2 + SiH_3Cl$	0.2 (0.17)	0.2 (0.14)	0.13 (0.09)	0.08 (0.06)	0.07 (0.06)
$SiHCl + SiH_2Cl_2 \rightarrow Si_2HCl_3 + H_2$	0.22 (0.18)	0.17 (0.14)	0.14 (0.1)	0.1 (0.08)	0.08 (0.06)
Multiple-Well, Multiple-Channel Reaction of the Ethyl Radical with Oxygen [first (entrance) well pertaining to the formation of the chemically activated moiety]					
$CH_3CH_2O\dot{O} \rightarrow C_2H_5\dot{O} + O$	0.11 (0.05)	0.11 (0.05)	0.10 (0.04)	0.06 (0.04)	0.05 (0.03)
$CH_3CH_2O\dot{O} \rightarrow C_2H_4 + HO_2$ (elimination)	0.17 (0.08)	0.2 (0.08)	0.13 (0.06)	0.13 (0.05)	0.10 (0.04)
Second Well Pertaining to the First Hydroperoxy Radical and β Scission Pathway					
$\dot{C}H_2CH_2OOH \rightarrow C_2H_4 + HO_2$ (β scission)	0.2 (0.10)	0.2 (0.09)	0.15 (0.08)	0.1 (0.05)	0.08 (0.02)
$\dot{C}H_2CH_2OOH \rightarrow$ (cy) $H_2COCH_2 + OH$	0.17 (0.08)	0.13 (0.06)	0.08 (0.04)	0.06 (0.02)	0.03 (0.01)
Third Well Pertaining to the Second Hydroperoxy Radical and Formation of Acetaldehyde					
$CH_3\dot{C}HOOH \rightarrow CH_3CHO + OH$	0. 15 (0.06)	0.13 (0.05)	0.06 (0.02)	0.06 (0.02)	0.01 (0.01)

[a] The numbers in parenthesis indicate average errors in the rate coefficient. Nomenclature: $m \times n$ means the Tchebycheff approximant has m basis functions along the temperature axis and n basis functions along the pressure axis, etc.

TABLE 3: Maximum Relative Errors in the Rate Coefficient over the Considered Temperature and Pressure Ranges for the Damped Pseudospectral Approximants with Master Equation Analysis of the Collisional Energy Transfer[a]

channel	6 × 3	5 × 4	7 × 3	6 × 4	8 × 3
Single-Well, Single-Channel Reaction $H + C_6H_5 \rightarrow C_6H_6$ with Allowance for Radiative Recombination					
$H + C_6H_5 \rightarrow C_6H_6$	0.11 (0.07)	0.08 (0.06)	0.06 (0.05)	0.03 (0.01)	0.01 (0.01)
Single-Well, Multiple-Channel Reaction of $SiHCl + SiH_2Cl_2$					
$SiHCl + SiH_2Cl_2 \rightarrow SiH_2 +$ SiHCl3	0.08 (0.04)	0.05 (0.03)	0.05 (0.03)	0.02 (0.01)	0.01 (0.01)
$SiHCl + SiH_2Cl_2 \rightarrow SiCl_2 + SiH_3Cl$	0.11 (0.12)	0.10 (0.10)	0.08 (0.06)	0.07 (0.04)	0.02 (0.01)
$SiHCl + SiH_2Cl_2 \rightarrow Si_2HCl_3 + H_2$	0.15 (0.11)	0.12 (0.1)	0.09 (0.07)	0.06 (0.04)	0.03 (0.01)
Multiple-Well, Multiple-Channel Reaction of the Ethyl Radical with oxygen [first (entrance) well pertaining to the formation of the chemically activated moiety]					
$CH_3CH_2O\dot{O} \rightarrow C_2H_5\dot{O} + O$	0.08 (0.03)	0.07 (0.03)	0.05 (0.02)	0.03 (0.02)	0.01 (0.01)
$\dot{C}H_3CH_2O\dot{O} \rightarrow C_2H_4 + HO_2$ (elimination)	0.1 (0.05)	0.1 (0.05)	0.08 (0.03)	0.05 (0.03)	0.02 (0.01)
Second Well Pertaining to the First Hydroperoxy Radical and β Scission Pathway					
$\dot{C}H_2CH_2OOH \rightarrow C_2H_4 + HO_2$ (β scission)	0.13 (0.06)	0.1 (0.06)	0.1 (0.05)	0.06 (0.03)	0.01 (0.01)
$\dot{C}H_2CH_2OOH \rightarrow$ (cy)$H_2COCH_2 + OH$	0.1 (0.06)	0.08 (0.04)	0.05 (0.02)	0.01 (0.01)	0.01 (0.01)
Third Well Pertaining to the Second Hydroperoxy Radical and Formation of Acetaldehyde					
$CH_3\dot{C}HOOH \rightarrow CH_3CHO + OH$	0.08 (0.05)	0.08 (0.04)	0.04 (0.02)	0.02 (0.01)	0.02 (0.01)

[a] The numbers in parentheses indicate average errors in the rate coefficient. Nomenclature: $m \times n$ means the damped pseudospectral approximant has m basis functions along the temperature axis and n basis functions along the pressure axis, etc.

TABLE 4: Limiting High-Pressure Rate Coefficients of the Reaction Channels in the Chemically Activated Reaction of $SiHCl + SiH_2Cl_2$[a]

reactions	log *A*	E
$SiHCl + SiH_2Cl_2 \rightarrow HCl_2SiSiH_2Cl$	11.7	6.8
$HCl_2SiSiH_2Cl \rightarrow SiHCl + SiH_2Cl_2$	13.6	46.9
$HCl_2SiSiH_2Cl \rightarrow SiH_2 + SiHCl_3$	14.1	51.3
$HCl_2SiSiH_2Cl \rightarrow SiCl_2 + SiH_3Cl$	14.1	49.6
$HCl_2SiSiH_2Cl \rightarrow Si_2HCl_3 + H_2$	14.3	53.5

[a] Rate constants in the form $A \exp(-E/RT)$. Prefactor, A, in s^{-1} for unimolecular reactions and in $cm^3/(mol\ s)$ for bimolecular reactions. Barriers, E, in kcal/mol.

Tables 1, 2, and 3 present the maximum and average errors of approximation for these channels incurred by the empirical approximants, the Tchebycheff approximants, and the damped pseudospectral approximants, respectively, for this system of reactions.

The third system is the multiple-well, multiple-channel reaction of the ethyl radical with oxygen. This chemically activated reaction occurs through three wells. The initial well corresponds to the chemically activated molecule $CH_3CH_2O\dot{O}$ formed by the radical addition process via a loose transition state. This activated molecule can further isomerize to the hydroperoxy radicals $\dot{C}H_2CH_2OOH$ and $CH_3\dot{C}HOOH$. Figure 1 depicts the potential energy diagram. Table 5 displays the limiting high-pressure rate coefficients for the various channels of this system. This system of reactions has been the topic of a recent comprehensive ab initio study[20] and a full master equation analysis[5,13] in conjunction with variational RRKM theory. The system exhibits the presence of competing channels for ethylene production in two different wells. Our treatment of the reaction mechanism allows decomposition back to reactants, reversible isomerization between the initial moiety and each of the hydroperoxy radicals, and irreversible dissociation of all of the moieties into products. All isomerizations proceed through tight transition states, but some decomposition reactions into products occur through loose transition states. The concentrations of the reactants are assumed to be infinitely dilute in a thermal bath of gaseous helium. The RRKM microcanonical rate coefficients for all of the reaction channels were computed to be functions of the total internal energy and the total angular momentum using the variational microcanonical theory of Forst.[21] In this method, the transition state properties are evaluated at the variational minimum of the integrated density of states along the reaction coordinate, but only with the knowledge of the limiting high-pressure rate coefficient and the reactant and product molecular parameters for each channel. The absolute

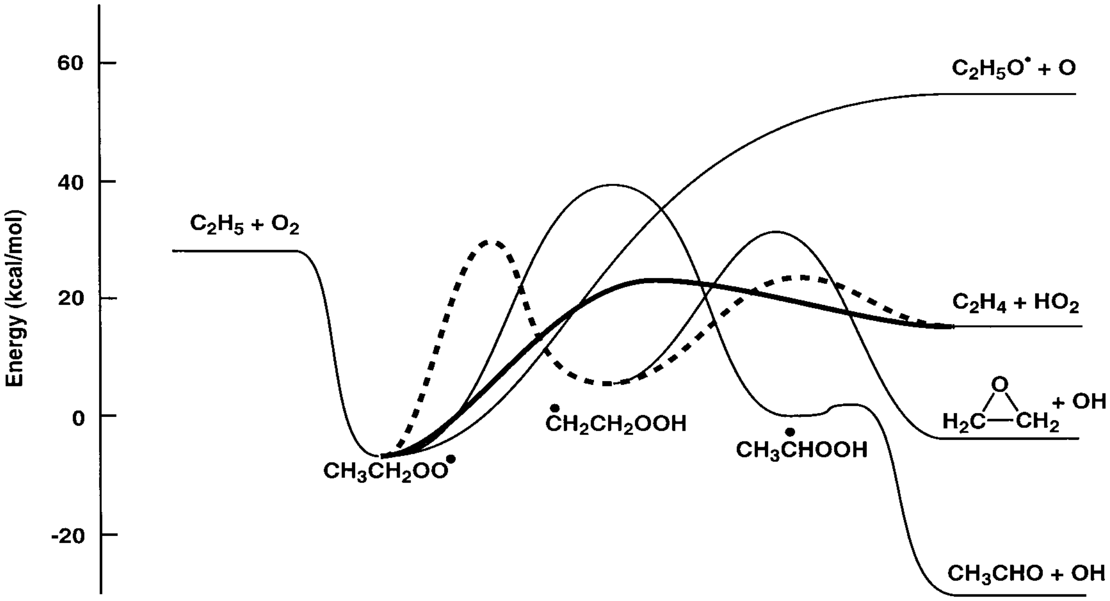

Figure 1. Potential energy diagram for the chemically activated reaction of the ethyl radical with oxygen.

TABLE 5. Limiting High-Pressure Rate Coefficients of the Reaction Channels in the Chemically Activated Reaction of the Ethyl Radical with Oxygen[a]

reactions	A	n	E
First (entrance) Well Pertaining to the Formation of the Chemically Activated Moiety			
$C_2H_5 + O_2 \rightarrow CH_3CH_2O\dot{O}$	3.00×10^{12}	0.000	−0.05
$CH_3CH_2O\dot{O} \rightarrow C_2H_5 + O_2$	4.14×10^{19}	−1.618	34.67
$CH_3CH_2O\dot{O} \rightarrow C_2H_5\dot{O} + O$	4.10×10^{14}	0.000	58.30
$CH_3CH_2O\dot{O} \rightarrow C_2H_4 + HO_2$ (elimination)	6.11×10^{6}	1.938	28.50
Second Well Pertaining to the First Hydroperoxy Radical and β Scission Pathway			
$CH_3CH_2O\dot{O} \rightarrow \dot{C}H_2CH_2OOH$	9.28×10^{5}	2.170	36.50
$\dot{C}H_2CH_2OOH \rightarrow CH_3CH_2O\dot{O}$	4.35×10^{6}	1.666	24.23
$\dot{C}H_2CH_2OOH \rightarrow C_2H_4 + HO_2$ (β scission)	1.07×10^{15}	−0.695	17.50
$\dot{C}H_2CH_2OOH \rightarrow$ (cy)H_2COCH_2 + OH	6.92×10^{11}	0.185	25.64
Third Well Pertaining to the Second Hydroperoxy Radical and Formation of Acetaldehyde			
$CH_3CH_2O\dot{O} \rightarrow CH_3\dot{C}HOOH$	2.58×10^{10}	0.782	45.10
$CH_3\dot{C}HOOH \rightarrow CH_3CH_2O\dot{O}$	9.34×10^{10}	0.260	37.35
$CH_3\dot{C}HOOH \rightarrow CH_3CHO + OH$	3.30×10^{13}	0.000	1.00

[a] Rate constants in the form $AT^n \exp(-E/RT)$. Prefactor, A, in s^{-1} for unimolecular reactions and in $cm^3/(mol\ s)$ for bimolecular reactions. Barriers, E, in kcal/mol.

rate coefficients of each of the channels were computed using the master equation treatment described in section 2; the full details of the numerical methods involved are given in ref 5 and 13. For this system, we have compared the various models of approximation over the wide temperature- and pressure ranges of 300−3000 K and 0.02−200 atm. Tables 1, 2, and 3 present the maximum and average errors of approximation for these channels incurred by the empirical approximants, the Tchebycheff approximants, and the damped pseudospectral approximants, respectively, for this system of reactions.

As can be seen from Table 1, the Lindemann-based methods perform well in some instances while in many instances they yield a relative error greater than 0.2, the threshold criterion of goodness of approximation. Furthermore, there are instances when they possess errors as high as 400%. Essentially, there does not appear to be a uniformity in the pattern of classification of approximation errors for these type of approximants. By far, the most accurate approximants are the damped pseudospectral approximants, more than even the Tchebycheff approximants. In general, these approximants are of higher accuracy than the Lindemann-based methods. They possess the property of uniform approximation over the entire temperature and pressure domains. Furthermore, over these domains, they minimize the maximum deviation of the true absolute rate constants from their approximated values. For a given number of basis functions along the temperature and pressure axes they possess the same number of coefficients while providing approximants of much higher accuracy than pure Tchebycheff approximants. A significantly useful feature of the Tchebycheff and the damped pseudospectral approximants is that they may be evaluated rapidly using the fast Fourier transform (FFT) by means of simple change of variables. This feature is particularly useful in the incorporation of such approximants in predictive reactor models in flame dynamics, microelectronics etching processes, and reactive computational fluid dynamics including turbulence models where approximants are repeatedly computed in simulation, optimization, and control calculations.

An important issue is the computational overhead incurred in incorporating full-pressure dependent parameterization into detailed chemical kinetic mechanisms. To make computational comparisons of the various parameterization schemes, a small elementary reaction mechanism was assembled and used to generate reactant and product concentration profiles over time. The mechanism is displayed in Table 5 along with the limiting high-pressure rate coefficient for each reaction. A simulation of the mechanism using the CHEMKIN-II package[22] was performed using four different parameterization schemes for incorporating the pressure dependence. The simulation was carried out for three different temperatures for a total simulation time duration of 50 ms. The stiffness of the differential equations will be a function of temperature, and therefore integration times will be longer for those temperatures at which there is a wider disparity in the time scales of the species dynamics. All computations were carried out on a Sun-Ultrasparc-2 workstation. Table 6 displays the computational times (CPU times) taken for the whole simulation; in the computations performed, the damped pseudospectral and Tchebycheff approximants were evaluated directly without any recourse to fast Fourier transformations. The damped pseudospectral scheme compares well in being computationally cost-effective. It requires only nominally more amount of time than the conventionally used Lindemann-based schemes of approximation and is vastly more

TABLE 6: Comparison of Simulation Times of a Model Detailed Chemical Kinetic Mechanism Using Different Parameterization Techniques

parameterization technique	time (μs) for simulation at 375 K	time (μs) for simulation at 775 K	time (μs) for simulation at 1575 K
Troe's F_{cent} method	0.579	0.603	0.558
Poole and Gilbert method	0.586	0.620	0.575
8 × 3 pure Tchebycheff approximant	0.627	0.670	0.602
8 × 3 damped pseudospectral approximant	0.663	0.699	0.620

accurate than the latter. It is possible to accelerate the evaluations of the damped pseudospectral approximants by the fast Fourier transformation but for the example chemical kinetic mechanism studied here it is not a necessity as it is small.

5. Summary

Damped pseudospectral approximants have been shown to be a reliable means for approximating the temperature- and pressure-dependent absolute rate constants of elementary gas-phase reactions over wide ranges of temperature and pressure. Their application has been demonstrated on the recombination reaction of radicals leading to benzene formation, taking into account effects of infrared stabilization, on a complex multiple-well, multiple-channel system of reactions pertaining to the reaction of the ethyl radical with oxygen as well as a single-well, multiple-well channel reaction in chemical vapor deposition. Absolute rate constants were generated using a master equation analysis with a variational RRKM computation of the microcanonical rate coefficients.

The accuracy of the damped-pseudospectral approximants is superior to that of Tchebycheff approximation; and in general they are far more accurate than Lindemann-based approximation methods. Theoretically they possess interesting properties. Similar to Tchebycheff polynomials, they minimize the maximum interpolation error among all polynomial basis functions. Moreover, the approximation error decreases faster than the total number of basis functions retained in their formalism. There exists an optimal number of basis functions corresponding to any arbitrarily specified threshold error for these types of approximants. Additionally, they allow the falloff surface, which is a function of temperature and pressure, to possess arbitrary discontinuities in any of its derivatives. Hence semisharp and sharp plateaus of the falloff surface may be captured accurately and with ease.

Most importantly, their computational costs and storage requirements are very attractive due to their being amenable to evaluation by the fast Fourier transform. Thus, these approximants are of immense importance in detailed chemical kinetic modeling of combustion[23] and chemical vapor deposition[11,12,24] among many other areas of chemical reaction analysis of the gas phase.

Last, we wish to mention that a robust computer code for the construction of the damped pseudospectral approximants and another one for constructing pure Tchebycheff approximants are available from the author upon request.

Acknowledgment. The author thanks Dr. Robert Burridge of Schlumberger-Doll Research for discussions on the mathematical aspects and Professor John Barker, Professor Joseph Bozzelli, and Dr. Anthony Dean for discussions on the aspects of chemistry.

References and Notes

(1) Marcus, R. A. *J. Chem. Phys.* **1952**, *20*, 359.
(2) Marcus, R. A. *J. Chem. Phys.* **1966**, *45*, 2630.
(3) Holbrook, K. A.; Pilling, M. J.; Robertson, S. H. *Unimolecular Reactions*; Wiley: London, **1996**.
(4) Venkatesh, P. K.; Dean, A. M.; Cohen, M. H.; Carr, R. W. *J. Chem. Phys.* **1997**, *107*, 21, 8904.
(5) Venkatesh, P. K.; Dean, A. M.; Cohen, M. H.; Carr, R. W. *J. Chem. Phys.* **1999**, *111*, 18, 8313.
(6) Gilbert, R. G.; Luther, K.; Troe, J. *Ber. Bunsen. Phys. Chem.* **1983**, *87*, 169.
(7) Poole, J. S.; Gilbert, R. G. *Int. J. Chem. Kinet.* **1994**, *26*, 273.
(8) Venkatesh, P. K.; Chang, A. Y.; Dean, A. M.; Cohen, M. H.; Carr, R. W. *AIChE J.* **1997**,*43*, 5, 1331.
(9) Griffel, D. H. *Applied Functional Analysis*; John Wiley: New York, 1981.
(10) Barker, J. R. *J. Phys. Chem.* **1992**, *96*, 7361
(11) Swihart, M. T. *Gas Phase Chemical Kinetics and the Detailed Modelling of Chemical Vapour Deposition Processes*, Ph.D. Thesis, Department of Chemical Engineering and Materials Science, University of Minnesota, Minneapolis, Minnesota; University Microfilms: Ann Arbor MI, 1997.
(12) Swihart, M. T.; Carr, R. W. *J. Phys. Chem. A* **1998**, *102*, 1542.
(13) Venkatesh, P. K. *Studies in Chemical Reaction Engineering*, Ph.D. Thesis, Department of Chemical Engineering and Materials Science, University of Minnesota, Minneapolis, Minnesota; University Microfilms: Ann Arbor MI, 1997.
(14) Pechukas, P.; Light, J. C. *J. Chem. Phys.* **1965**, *42*, 3281.
(15) Quack, M.; Troe, J. *Ber. Bunsen. Phys. Chem.* **1974**, *78*, 240.
(16) Eliason, M. A.; Hirschfelder, J. O. *J. Chem. Phys.* **1959**, *30*, 1426.
(17) Miller, W. H. *J. Phys. Chem. A* **1998**, *102*, 5, 793.
(18) Pilling, M. J. *Annu. Rev. Phys. Chem.* **1996**, *47*, 81.
(19) Cheney, E. W. *Introduction to Approximation Theory*, 2nd ed.; Chelsea: New York, 1982.
(20) Ignatyev, I. S.; Xie, Y.; Allen, W. D.; Schaefer, H. F., III. *J. Chem. Phys.* **1997**, *107*, 1, 141.
(21) Forst, W. *J. Phys. Chem.* **1991**, *95*, 3612.
(22) Kee, R. J.; Rupley, F. M.; Miller, J. A. *Chemkin-II A Fortran Chemical Kinetics Package for the Analysis of Gas-Phase Chemical Kinetics"*, SAND89−8009 UC 401, Sandia National Laboratories, 1989.
(23) Westbrook, C. K.; Dryer, F. L. *Prog. Energy Combust. Sci.* **1984**, *10*, 1.
(24) Ern, A.; Giovangigli, V; Smooke, M. D. *J.Comput. Phys.* **1996**, *126*, 21.